


## SURGICAL TECHNIQUE

# Arthroscopic Superior Capsule Reconstruction and Rotator Cuff Repair to Restore Static and Dynamic Stability of the Shoulder

Yamuhanmode Alike, PhD<sup>1</sup> , Jing-yi Hou, MD<sup>2</sup>, Yi-yong Tang, MD<sup>3</sup>, Meng-lei Yu, MD<sup>1</sup>, Yi Long, MD<sup>2</sup>, Fang-qi Li, MD<sup>2</sup>, MaslahIdiris Ali, MD<sup>2</sup>, Hao Yuan, MD<sup>2</sup>, Rui Yang, MD<sup>2\*</sup>

Department of <sup>1</sup>Emergency and <sup>2</sup>Orthopaedic Surgery, Sun Yat-sen Memorial Hospital, Sun Yat-sen University, Guangzhou and <sup>3</sup>Department of Orthopaedic Surgery, The Eighth Affiliated Hospital of Sun Yat-sen University, Shenzhen, China

**Objective:** Treatment of massive irreparable rotator cuff tears (RCT) has shown limited clinical success and a variety of subsequent complications. Superior capsule reconstruction (SCR) has been proved to reestablish superior stability but does not restore the dynamic force or shoulder kinematics. There are numerous reports of the short-term failure of SCR grafts at the glenoid side, which relate to the non-biological healing of grafts. To restore both dynamic and static stability and to provide biologic augmentation, an integrated procedure for massive irreparable RCT using an Achilles tendon–bone allograft (ATBA) was developed.

**Method:** This was a retrospect study completed between October 2019 and April 2020. A 71-year-old woman with massive and irreparable rotator cuff tears was enrolled in our study. The ATBA was folded into a double-layer structure. The superior layer (proximal portion) served as a bridge patch to dynamic the glenohumeral joint, while the inferior layer (distal portion) served as the superior capsule to restore static stability of glenohumeral joint. To enhance biologic healing on the glenoid side, we fixed the calcaneus of the graft on the superior–posterior side of the superior glenoid rim. The recovery of shoulder function (including strength, range of motion, acromiohumeral interval, and fatty infiltration) was assessed at 6 months postoperation.

**Result:** At 6-month follow-up, the patient's strength had improved significantly (from abduction of grade 3 preoperatively to grade 4 at 6 months). Radiographic analysis showed an increase in the acromiohumeral interval from 3 to 7 mm. Magnetic resonance imaging revealed an intact graft, with the thickness of the ligament part maintained (at 6–7 mm). Most importantly, recovery of atrophy and fatty infiltration of the supraspinatus were observed. No graft tears were observed on the glenoid side.

**Conclusion:** This technique could provide a preferable treatment option by restoring shoulder kinematics and augmentating biological healing for patients with massive irreparable RCT.

**Key words:** Integrated repairment; Rotator cuff tear; Static and dynamic stabilizer; Superior capsule reconstruction

## Introduction

Massive rotator cuff tears (RCT) have been historically considered tears with a diameter  $\geq 5$  cm and/or that are involved in the detachment of at least two entire tendons<sup>1, 2</sup>. An irreparable RCT is defined as a tear is unable to

be reapproximated to its insertion on the tuberosities despite application of conventional release techniques, due to the degeneration, retraction, and fatty infiltration of cuff tissue<sup>3, 4</sup>. A recent systematic review identified that 42% of RCT can be classified as irreparable tears<sup>5</sup>. Although various surgical

**Address for Correspondence** Rui Yang, MD, Department of Orthopaedic Surgery, Sun Yat-sen Memorial Hospital, Sun Yat-sen University, 107# Yan Jiang Road West, Guangzhou, Guangdong Province, China 510120 Tel:+86 136 9420 0667; Fax: +86-020 -81332496; Email: yangr@mail.sysu.edu.cn

**Disclosure:** The authors declare no conflict of interest.  
Received 4 June 2020; accepted 9 July 2020

techniques have been developed and applied, postoperative complications and uncertain outcomes often trouble both clinicians and patients<sup>6</sup>. Galatz *et al.*<sup>7</sup> report that the re-tear rate of massive irreparable RCT could be up to 94%. Although tendon transfer provides an alternative option for younger patients, narrow surgical indications limit its use<sup>8</sup>. Reverse total shoulder arthroplasty is only suitable for elderly patients with severe glenohumeral joint arthritis<sup>9</sup>.

In 2013, Mihata *et al.*<sup>10</sup> described the arthroscopic superior capsule reconstruction (SCR) with *fascia lata* autograft for massive RCT. Favorable outcomes have been reported, including significant improvements in pain and range of motion in the shoulder. Further techniques have evolved to obviate the need for *fascia lata* autograft use and reduce graft site morbidity<sup>11</sup>. However, high re-tear rates at the glenoid side have been frequently reported during medium-term follow-up<sup>12</sup>. In addition, in some cases, the humeral head migrated superiorly again because of the “creep” (graft get stretched) phenomenon, which results in increased joint laxity, and may lead to SCR failure<sup>13</sup>. Although the importance of restoring the remnant rotator cuff tissue to maximize clinical outcomes when performing SCR has been highlighted<sup>14, 15</sup>, problems such as extreme tension at the suture site, high re-tear rates, and incomplete dynamic function recovery after SCR still exist.

Herein, we describe the incorporation of SCR with rotator cuff repair using an integrated Achilles tendon–bone allograft (Osteorad Biomed, Shanxi, China). The aim is to restore the normal anatomical structure and kinematics of the glenohumeral joint. We speculated that the static stabilizer (superior capsule) would shorten the acromion–humeral interval (AHI), which would allow repairing of the remnant rotator cuff under a lower tension. By providing a primary restraint to the proximal migration of the humerus, the reconstructed superior capsule would protect the cuff tissue from excessive stress. In contrast, as the function of the dynamic stabilizer (rotator cuff tissue) recovers, it might help in reducing the graft creep.

## Surgical Technique

### Indication

The ideal candidates for this procedure were RCT with the following conditions: (i) tendons for which release techniques were unable to restore the native footprint; (ii) tendons with slight fatty atrophy (evaluated as grade IV based on Goutallier classification using MRI); (iii) a decreased AHI with or without acetabularization of the acromion (evaluated as grade IV based on Hamada classification using plain radiography); and (iv) previous failures of patch bridging and SCR. The exclusion criteria include: (i) severe joint deformities; (ii) a static anterior dislocation or subluxation of the glenohumeral; and (iii) cervical nerve palsy or deltoid dysfunction, and infection.

Our case is a 71-year-old woman who presented with a 2-month history of right shoulder pain and weakness. She

had no history of right shoulder injury or trauma. On physical examination, her active abduction was 36.7°, forward flexion 37.8°, external rotation with the arm to the side was 38°, and internal rotation was to the T<sub>12</sub> level. A positive drop arm sign was observed, and a negative result in assessing deltoid function (including the swallow tail test, the deltoid extension lag test, and the Bertelli test). Plain radiographs demonstrated no evidence of osteoarthritis, but the AHI was approximately 3 mm (Hamada classification 2). The MRI revealed a full-thickness rotator cuff tear of the supraspinatus, and the retracted supraspinatus was typically medial to the glenoid. In addition, there was as much fatty degeneration of the supraspinatus as there was muscle

### Patient Positioning and Portal Setup

The procedure was performed with the patient in a lateral decubitus position with general anesthesia and a single shot of interscalene block. The operative arm was examined to

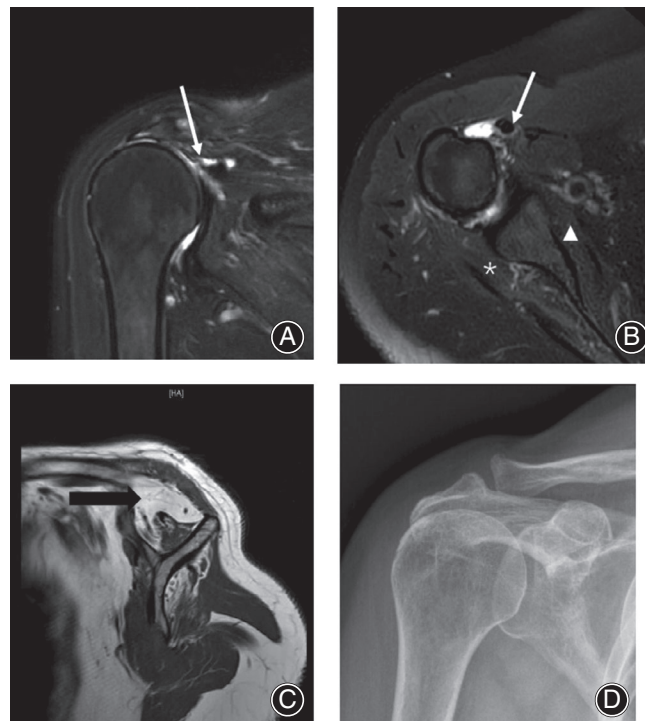


**Fig. 1** Preoperative radiography of right shoulder. (A) T2-weighted oblique sagittal plane MRI showing a massive rotator cuff tear. The supraspinatus (white arrow) has retracted to the medial side of the glenoid. (B) T2-weighted oblique sagittal plane MRI showing dislocation of the long head of the bicep tendon (white arrow), and muscle atrophy of the subscapularis (white triangle) and infraspinatus (white arrow). (C) T1-weighted oblique sagittal plane MRI showing the supraspinatus with fatty infiltration (Goutallier stage 3). (D) Standing anterior–posterior (AP) radiograph of the right shoulder, with acromiohumeral interval <5 mm, without acetabularization of acromion.

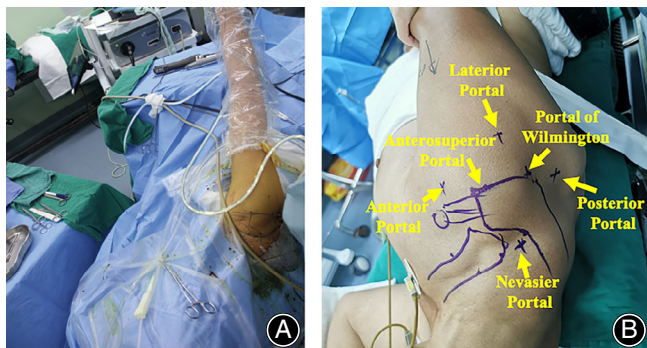


**Fig. 2** The arm is positioned in the standard lateral decubitus position (A). Routine portals are used during the procedure on the right shoulder: anterior portal, anterosuperior portal, lateral portal, portal of Wilmington, posterior portal, and Nevasier portal (B).

assess the range of motion, and was placed at 45° abduction, 15° forward flexion, and natural rotation. The portals were similar to those used for routine shoulder arthroscopy: posterior, anterior, lateral, anterosuperior, posterosuperior, and Nevasier portals. The lateral portalis was used as the graft introduction portal (Fig. 2).

#### Arthroscopic Evaluation and Preparation

Diagnostic arthroscopy was routinely performed in the glenohumeral and subacromial space to determine the tissue quality of the rotator cuff, the long head tendon of the biceps (LHBT), the labrum, and the cartilage. We removed the synovitis around the subscapularis. The coracohumeral ligament was then mobilized through release techniques. After a bursectomy was performed around the subcoracoid, the subscapularis and the supraspinatus tendon were released, and their integrity and mobility were assessed.

In this case, we arthroscopically confirmed a partial tear of the superior third of the subscapular tendon (Lafosse type I), and LHBT dislocation resulting from a complete lesion of the anterior-posterior pulley structure. The extent of the tear of the supraspinatus tendons was more than 5 cm, which was not able to advance to the native footprint despite a release technique. A suprascapular nerve release is performed when compression is suspected (Fig. 3A). For the biological healing of the lateral side of the graft to the humeral footprint, microfracture was performed using an awl (Condropick, Arthrex, Naples, FL, USA) at the tip perpendicular to the footprint. After that, decortication of the superior glenoid rim was performed to provide a bleeding bed to promote bone-to-bone healing between the superior glenoid rim and the graft. Then, a 3.5-mm diameter drill hole was made at the center of the bleeding bed as well as the bone part of the graft, with the aid of a guidewire passed through the acromion (Fig. 3B).

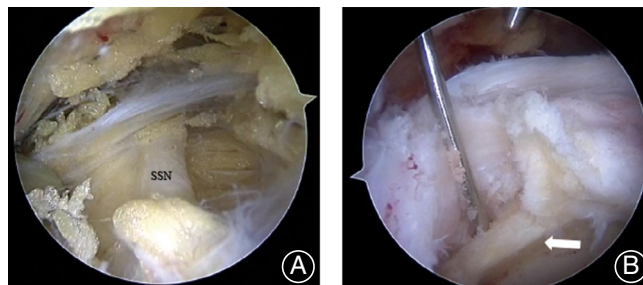


**Fig. 3** Releasing the suprascapularis nerve (A) and preparing the bleeding bed and drill hole on the superior glenoid rim for the calcaneus part of the graft fixation (B).

#### Anchor Placement for Subscapularis and Infraspinatus Fixation

For the subscapularis fixation, a 4.5-mm anchor (Twinflix; Smith & Nephew) was placed at the intertubercular groove of the humeral head. One of the sutures was used for fixation of the proximal part of the subscapularis tendon, and another was passed out of the lateral portal. For the infraspinatus fixation, a 4.5-mm anchor (BioComposite Corkscrew FT; Arthrex) was placed at the posterior margin of the footprint as a goalpost anchor. One of the sutures was used for the partial infraspinatus fixation, and another was passed out of the posterior portal.

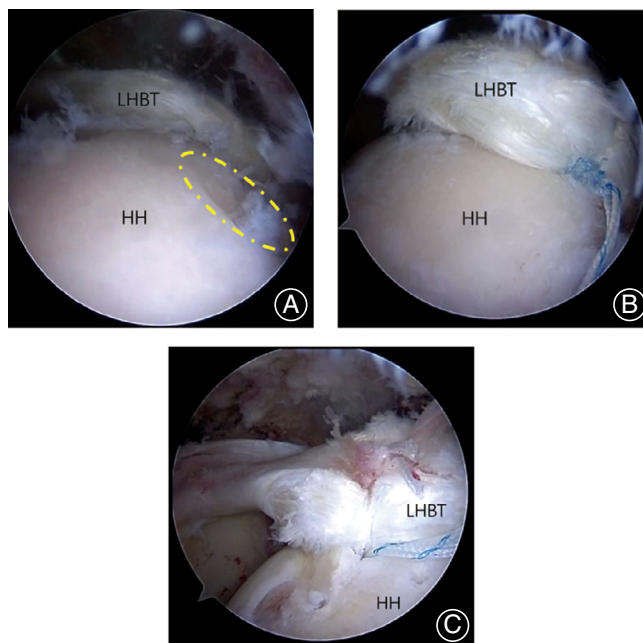


**Fig. 4** The long head of bicep tendon rerouting (LHBT). (A) Releasing the LHBT (black arrow) before rerouting it to the anterior margin of the supraspinatus insertion (dotted yellow line). (B) The rerouted LHBT with anteroinferior (B) and posterosuperior (C) portion fixed on the humeral head (HH).



**Long Head of Bicep Tendon Rerouting**

The LHBT rerouting procedure largely mimicked the method described by Kim *et al.*<sup>16</sup>. To make up for the insufficient width of the graft, we rerouted the proximal part of the LHBT and securely fixed it onto the humeral head as an anterior part of the superior capsule. We removed the soft tissue around the LHBT, and an abrasion of the posterior wall of the groove was performed. Then the LHBT was posteriorly repositioned to the anterior margin of the greater tuberosity (GT) of the humeral head (Fig. 4A). After the LHBT was rerouted, the third double-suture anchor (4.5 mm, Twinfix, Smith & Nephew) was placed at the anterior margin of the supraspinatus tendon insertion as the anterior goalpost anchor. One of the sutures was used to fix the posterosuperior part of the LHBT, and the remainder was passed out of the lateral portal. The anteroinferior

portion of the LHBT was securely fixed by the previous suture from the first anchor (Fig. 4B).

**Graft Preparation**

Graft dimensions were obtained medially on the superior glenoid rim, laterally on the humeral footprint between the remnant rotator cuff tissue, and anteriorly and posteriorly between the subscapularis and residual infraspinatus (Fig. 5).

The graft was sized to the appropriate dimension on the back table (Fig. 6, Table 1). A modified Ivan Wong<sup>17</sup> technique was performed. Four different colors of short-tailed interference knots (STIK) were prepared by tying mulberry-type knots over a Wissinger rod. The insertion points were marked with a surgical pen at 5 mm medial to the proximal margin of the graft. The STIK sutures were then passed through the graft, and a “road map” was drawn to help avoid confusion later. Then a drill hole (diameter = 3.5 mm) was prepared at the center of the calcaneal part of the graft for the fixation onto the superior glenoid rim. Before the graft was folded into a double-layer structure, a groove (3.0 mm × 1.5 mm) was made at the midline of the graft to help fold more smoothly (Fig. 7).

As the graft was folded, the superior layer was bridge repaired with the remnant supraspinatus tissue *via* the previous STIK. The medial of the inferior layer part is fixed by the calcaneal bone on the glenoid rim. The lateral part was used to reconstruct the footprint of the supraspinatus and the superior capsule on the humeral head. In this case, the

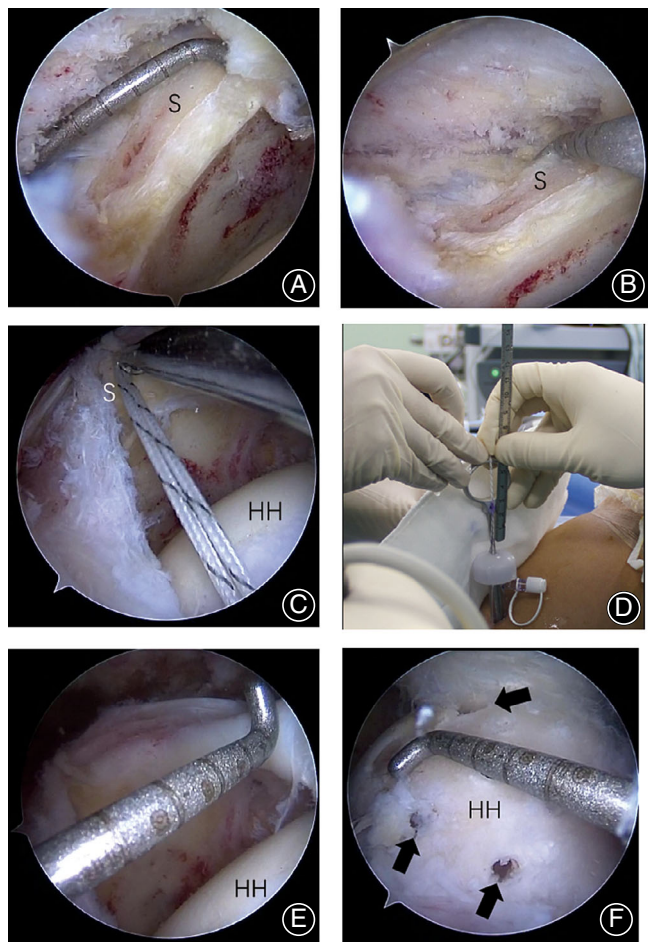


**Fig. 5** Preparation of the glenoidhumeral joint. (A, B) Measurement of the length (A) and width (B) of the bleeding bed on superior glenoid rim (S). (C, D) Measurement of the distance between the medial margin of the footprint and the superior glenoid rim. (E, F) Measurement of the width of the cuff defect (E) and the size of the footprint on the humeral head (HH) (F).

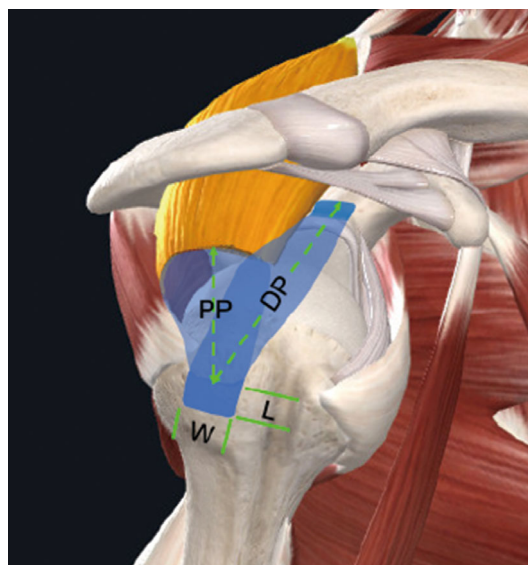


**Fig. 6** This diagram demonstrates the superior capsule reconstruction incorporated with rotator cuff repair with an Achilles tendon-bone allograft (ATBA). The dimension of the ATBA graft: the length (L) and width (W) of the humeral footprint, the distance from medial margin of the footprint to the remnant rotator cuff (PP), and the bleeding bed of the superior glenoid rim (DP).

**Table 1** Dimensions of the ATBA graft

The ATBA graft	Length (mm)	Width (mm)	Thick (mm)
Proximal portion (PP)	28	20	4
Middle portion (fold area)	20	15	5
Distal portion (DP)	40	22	4
Calcaneus	15	22	4

ATBA, Achilles tendon–bone allograft.

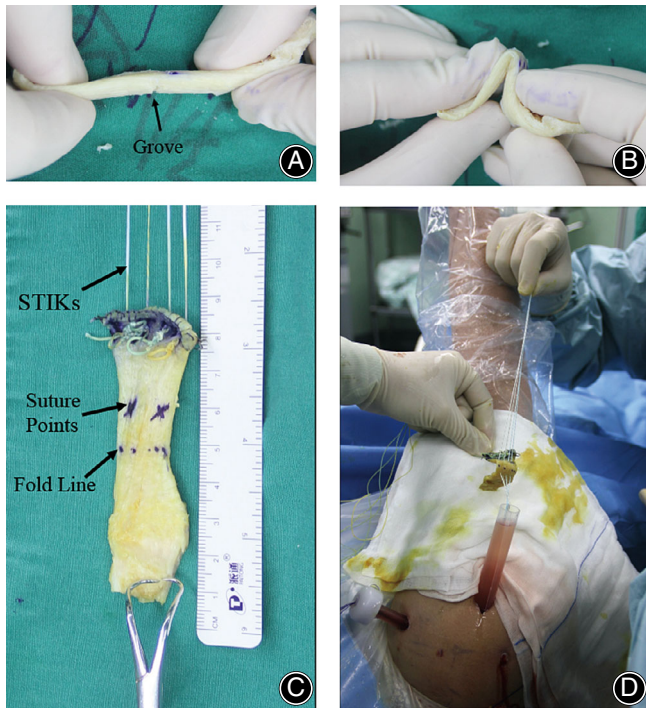


**Fig. 7** The Achilles tendon–bone allograft (ATBA) graft preparation. (A, B) A groove is made at the midline of the graft to help it fold into a double-layer structure. (C) Image of the ATBA after passage of the short-tailed interference knot suture. (D) The graft slid with the sutures from goalpost anchors and passed through a semi-open cannula at the lateral portal.

suture point of the medial row anchor was placed at 25 mm medial to the lateral margin of the graft.

### Graft Passage and Fixation

We sequentially passed the free ends of the sutures from two previously inserted goalpost anchors through the medial row suture point of the graft. These suture limbs were used as pulleys to introduce the graft into the joint. The graft was then passed through a semi-open cannula *via* the lateral portal, wherein the graft was “pushed” into the subacromial space (Fig. 7).

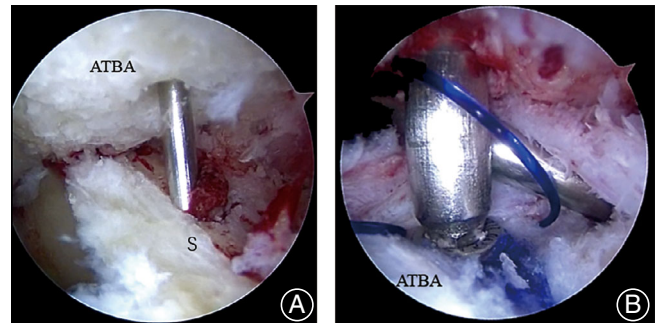


**Fig. 8** A hollow screw was led by the Kirschner wire and fixed the calcaneal part of the Achilles tendon–bone allograft (ATBA) graft onto the superior glenoid rim (S).

Then the arthroscope was reconfigured to the glenohumeral space to perform the graft fixation. The Neviaser portal is not an ideal option in this procedure, because it might penetrate the articular surface when placing a screw for graft fixation. Therefore, a Kirschner wire was sequentially percutaneously passed through the acromion, the drill hole of the graft, and the superior glenoid rim. Then a hollow screw (4.5 mm × 40 mm, Ideal Medical) was led by the Kirschner wire and we fixed the calcaneal part of the graft onto the superior glenoid rim (Fig. 8).

After fixation of the medial side of the graft, we inserted a rod into two layers of the graft to achieve temporary fixation of the lateral side of the graft onto the GT. Then we sequentially passed the free end of the STIK sutures around the cuff using a shuttle relay technique: two sutures through the supraspinatus and two through the infraspinatus. Knots were tied and tensioned on the top of the graft.

We attached the lateral part of the graft to the GT to keep it fully covered in the microfracture zone and tensioned it on the top of humeral head. Then we retrieved each suture limb from the goalpost anchors through the lateral portal and tied knots on the top of graft to finish the medial row fixation. Their suture tails were kept long enough to allow additional lateral row fixation. For the lateral row fixation, two 4.75-mm anchors (BioComposite Swive Lock C Vented, Arthrex) were placed at the anterior and posterior of the lateral margin of the footprint, respectively. We then took each



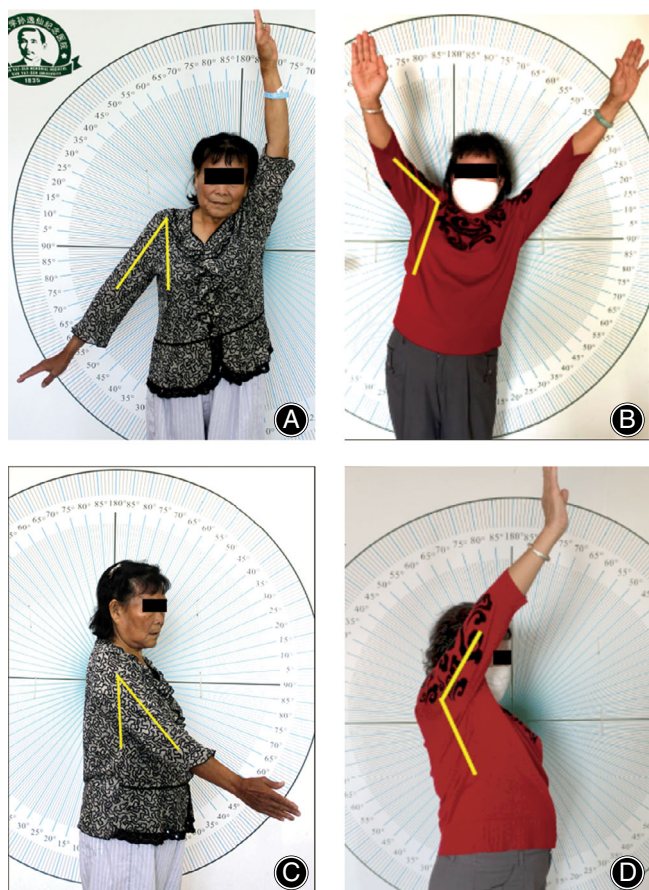


**Fig. 9** Strength as well as range of motion improved significantly (abduction/forward flexion, of 36.7°/37.8° preoperatively to 119°/132° at 6-month follow-up).

suture limb of these anchors to complete the suture bridge fixation. As this was performed, we added side-to-side sutures between the graft and the remnant cuff tissue to improve force coupling in the shoulder joint.

#### Final Testing and Concomitant Procedures

Once all the sutures were tied, the arthroscope was reconfigured to inspect the subacromial and glenohumeral space. The shoulder was then taken through a full range of motion to ensure there were no signs of impingement. As a consequence, the graft was fully attached to the top of the humeral head in a double-layer structure. The superior layer of the graft was sutured with the remnant rotator cuff tissue to act as a rotator cuff patch. The inferior layer of the graft covered the humeral head to act as an SCR, and was medially fixed by a calcaneal bone on top of the glenoid rim. The lateral part of the graft was attached to the humeral footprint using the classical double-row suture bridge technique. Compared with preoperative radiographs, our patient's immediate postoperative radiograph showed that the AHI has increased from 3 to 7 mm.

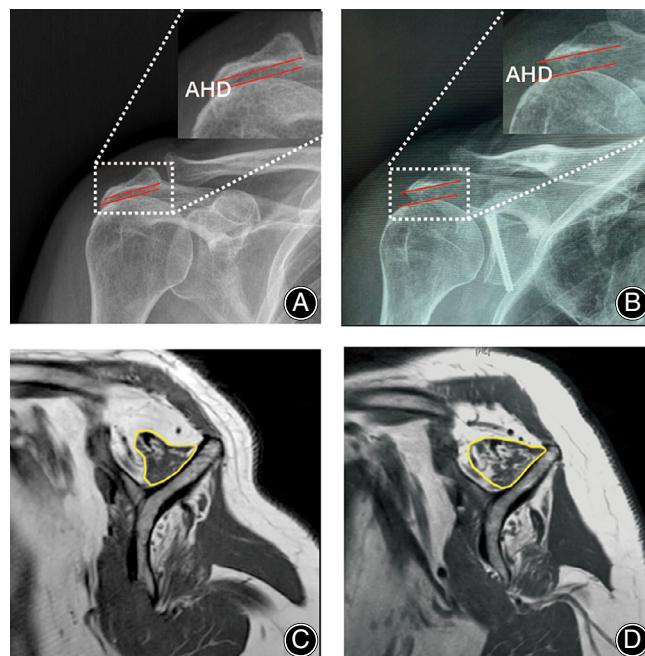


**Fig. 10** Radiographic analysis showed an increase in acromioclavicular interval from 3 mm preoperatively (A) to 7 mm postoperatively (B). T1-weighted oblique sagittal plane MRI showed significant recovery of muscular atrophy in the supraspinatus tendon: preoperation (C) and at 6-month follow-up (D). The yellow curve shows the cross-section area of the supraspinatus.

#### Postoperative Care and Rehabilitation

For postoperative pain control, we always place an epidural catheter (Epidural Minipack, 18-gauge; Portex, Keene, NH, USA) before finishing the operation. The catheter is placed *in situ* near the suprascapular nerve under direct visual control. Ropivacaine (2 mg/mL) was infused continuously at a rate of 3 mL/h by a mechanical infusion pump, maintained for 48 hours. Postoperatively, the patient's arm was supported in an abduction sling for 8 weeks before a limited and protected passive range of motion was allowed. Active-assisted elevation exercise was allowed at 12 weeks, and gentle strengthening was allowed from 16 weeks on.

#### Results

At 6-month follow-up, the patient's strength as well as her range of motion had improved significantly, and no subacromial impingement was observed (Fig. 9). Radiographic analysis showed an increase in the acromioclavicular interval from 3 mm to 7 mm and a successful fusion at the allograft–host junction. The MRI revealed an intact graft with the thickness of the ligament part maintained (6–7 mm) at 6 months postoperatively. Most importantly, a recovery of atrophy and fatty infiltration of the supraspinatus were observed. No sign of graft tears was observed on the glenoid side (Fig. 10).

## Discussion

Our case was classified as a massive irreparable RCT based on the definition described above<sup>1-4</sup>. Previous clinical reports have documented that repair of this kind of RCT should involve the restoration of both cuff and capsule anatomy to maximize clinical outcomes. The technique has been referred to as “functional biologic augmentation” or “over-the-top repair”. This procedure has been described as having the goal of decreasing the AHI to allow the rotator cuff to be stretched to reach the native attachment site<sup>14, 15</sup>. However, we noticed the phenomenon that, in some cases, after the release technique and even SCR was performed, the remnant cuff tissue could not be reapproximated to its native footprint.

### *Dynamic and Sciatic Stabilizer Reconstruction and Biologic Augmentation*

Shoulder function is maintained through the restoration of the superior capsule integrity and reestablishment of the rotator cuff tissue. It is, therefore, critical to anatomically restore the normal attachments of both the superior capsule and the rotator cuff on the humeral footprint. To achieve this, we developed an integrated surgical approach for the treatment of massive irreparable RCT. We hypothesize that this procedure is superior by allowing the graft to serve the following purposes.

#### *Restoring the Anatomical Structure of Both the Supraspinatus and the Capsule*

Anatomical studies have reported that the lateral side of the supraspinatus tendon is continuous with the humeral insertion of the superior capsule<sup>18, 19</sup>. On this basis, we developed the graft for SCR and the rotator patch in an integrated way, instead of as two isolated structures.

#### *Providing Nutrition for the Healing Process*

In Andary *et al.*<sup>20</sup>, 41% of the blood supply of the superior capsule originated from the anterior part of the rotator cuff; therefore, separation of the rotator cuff from the capsule would significantly disrupt the blood supply of the capsule, which could lead to failure of SCR. Therefore, restoring the coverage of rotator cuff tissue might enhance the vascularization and biological healing of the graft.

#### *Restoring the Function of Dynamic and Static Stabilizers*

The shoulder's ability to move without the risk of dislocation mainly relies on the incorporation of dynamic (rotator cuff) and static (superior capsule) stabilizers<sup>21</sup>. A simple SCR or RCT repair could not completely restore the natural anatomical structure of the shoulder joint, which is highly related to the graft creep (stretched and deformed)<sup>22</sup>. Thereby, we hypothesized that this procedure would provide sufficient static stability by reconstructing the superior capsule with the inferior layer of the graft, which would protect the rotator cuff tissue by reducing superior translation of the humeral head. The upper part of the graft, suture bridged

with the remnant cuff tissue, would extend of the shoulder joint with a synergistic contraction of deltoid muscle and reduce graft creep. Finally, an optimized functional recovery might be achieved by merging the synergistic benefits from these two critical stabilizers.

### *Disadvantages and Advantages of the Achilles Tendon-Bone Allograft Graft*

The inherent limitations of allograft such as the potential transmission of infectious diseases, infection, and possible immune reaction have been major impediments of the incorporation of allograft tissue. Despite this, Achilles tendon allografts have been successfully applied in tendon and ligamentous reconstructions throughout the body, including anterior cruciate ligament and posterior cruciate ligament reconstruction, and distal biceps repair<sup>23-25</sup>. To the best of our knowledge, implementation of an Achilles tendon allograft for SCR and rotator cuff repair in an integrated way has not been previously described. Unlike dermal patches, the ATBA could provide bone-to-bone healing on the superior glenoid rim side, and the natural bone-tendon transitional region of the ATBA made it to be an ideal graft for this procedure. In addition, the cuff-like structure of the ATBA results in a superior ability of cell induction and vascular ingrowth in the healing process. Most importantly, we are optimistic about our early finding: increased shoulder function and an intact graft with good fusion at the graft-host junction, which indicated that the ATBA could provide the opportunity for graft incorporation. We are examining clinic cases to further understand the potential long-term outcomes of this procedure.

### *Pitfalls and Pearls of the Integrated Achilles Tendon-Bone Allograft Technique*

The primary disadvantage of our procedure is the challenging surgical technique. Accurate evaluation and preoperative design are critical for this procedure. Every single detail, including the suture management to avoid suture entanglement intraoperatively, is critical to shorten the time of the surgery. In addition, arthroscopically untangling and fixing the graft in the limited field of vision and working space pose an enormous challenge to even expert surgeons with years of experience in arthroscopy.

Nevertheless, this procedure offers an alternative option for the treatment of patients with massive irreparable RCT, which can lead to good clinical results if patients with proper indications are selected. In this study, the patient was unwilling to undergo reverse shoulder arthroplasty (RSA) due to concerns about prosthesis loosening and the expense. Despite the patient being older, arthroscopic repair was still a preferable choice in this case considering the degree of the massive irreparable RCT. As arthroscopic rotator cuff repair has made rapid progress in recent years, it could be predicted that more favorable outcomes will be reported in middle-term or long-term follow-up. Most importantly, the patient

had recovered from pseudoparalysis 6 months postoperatively. Revision arthroplasty remains an option, if RSA is necessary.

In summary, this surgical approach involves combined application of the main available techniques, including partial repair, bridge patch, LHBT rerouting, SCR, and suprascapular nerve release. The purpose of this report is not the surgical technique itself, but the clinician's endless

pursuit and tireless efforts to restore the anatomical structure of the shoulder. Both anatomical and functional recovery of the shoulder joint were achieved.

### Acknowledgments

This study was supported by the National Natural Science Foundation of China (Grant No. 81972067).

### References

- Novi M, Kumar A, Paladini P, Porcellini G, Merolla G. Irreparable rotator cuff tears: challenges and solutions. *Orthop Res Rev*, 2018, 10: 93–103.
- Gerber C, Fuchs B, Hodler J. The results of repair of massive tears of the rotator cuff. *J Bone Joint Surg Am*, 2000, 82: 505–515.
- Dines DM, Moynihan DP, Dines J, McCann P. Irreparable rotator cuff tears: what to do and when to do it; the surgeon's dilemma. *J Bone Joint Surg Am*, 2006, 88: 2294–2302.
- Merolla G, Chillemi C, Franceschini V, et al. Tendon transfer for irreparable rotator cuff tears: indications and surgical rationale. *Muscles Ligaments Tendons J*, 2014, 4: 425–432.
- Mall NA, Lee AS, Chahal J, et al. An evidenced-based examination of the epidemiology and outcomes of traumatic rotator cuff tears. *Art Ther*, 2013, 29: 366–376.
- Maillot C, Martelloto A, Demezon H, Harly E, Le Huec J-C. Multiple treatment comparisons for large and massive rotator cuff tears: a network meta-analysis. *Clin J Sport Med off J Can Acad Sport Med*, 2019. <https://doi.org/10.1097/JSM.0000000000000786>. [Epub ahead of print.]
- Galatz LM, Ball CM, Teefey SA, Middleton WD, Yamaguchi K. The outcome and repair integrity of completely arthroscopically repaired large and massive rotator cuff tears. *J Bone Joint Surg Am*, 2004, 86: 219–224.
- Kanatli U, Özer M, Ataoğlu MB, et al. Arthroscopic-assisted latissimus Dorsi tendon transfer for massive, irreparable rotator cuff tears: technique and short-term follow-up of patients with pseudoparalysis. *Art Ther*, 2017, 33: 929–937.
- Kolade OO, Ghosh N, Fernandez L, et al. Study of variations in inpatient opioid consumption after total shoulder arthroplasty: influence of patient- and surgeon-related factors. *J Shoulder Elbow Surg*, 2019, 29: 508–515.
- Mihata T, Lee TQ, Watanabe C, et al. Clinical results of arthroscopic superior capsule reconstruction for irreparable rotator cuff tears. *Arthrosc - J Arthrosc Relat Surg*, 2013, 29: 459–470.
- Woodmass JM, Wagner ER, Borque KA, Chang MJ, Welp KM, Warner JJP. Superior capsule reconstruction using dermal allograft: early outcomes and survival. *J Shoulder Elbow Surg*, 2019, 28: S100–S109.
- Denard PJ, Brady PC, Adams CR, Tokish JM, Burkhart SS. Preliminary results of arthroscopic superior capsule reconstruction with dermal allograft. *Art Ther*, 2018, 34: 93–99.
- Ding S, Ge Y, Zheng M et al. Arthroscopic superior capsular reconstruction using "Sandwich" patch technique for irreparable rotator cuff tears. *Arthrosc Tech*, 2019, 8: e953–e959.
- Cabarcas BC, Garcia GH, Gowd AK, Liu JN, Romeo AA. Arthroscopic superior capsular reconstruction and over-the-top rotator cuff repair incorporation for treatment of massive rotator cuff tears. *Arthrosc Tech*, 2018, 7: e829–e837.
- Pennington WT, Chen SW, Bartz BA, Pennington JM. Superior capsular reconstruction with arthroscopic rotator cuff repair in a "functional biologic augmentation" technique to treat massive atrophic rotator cuff tears. *Arthrosc Tech*, 2019, 8: e465–e472.
- Kim YS, Lee HJ, Park I, Sung GY, Kim DJ, Kim JH. Arthroscopic in situ superior capsular reconstruction using the long head of the biceps tendon. *Arthrosc Tech*, 2018, 7: e97–e103.
- John R, Coady CM, Wong I. Revision of a failed latissimus Dorsi transfer for a massive rotator cuff tear with arthroscopic anatomic bridging reconstruction using an acellular human dermal matrix allograft. *Arthrosc Tech*, 2019, 8: e1171–e1179.
- Nimura A, Kato A, Yamaguchi K, et al. The superior capsule of the shoulder joint complements the insertion of the rotator cuff. *J Shoulder Elbow Surg*, 2012, 21: 867–872.
- Paufenberger L, Heuberger PR, Dyrna F, et al. Double-layer rotator cuff repair: anatomic reconstruction of the superior capsule and rotator cuff improves biomechanical properties in repairs of delaminated rotator cuff tears. *Am J Sports Med*, 2018, 46: 3165–3173.
- Andary JL, Petersen SA. The vascular anatomy of the glenohumeral capsule and ligaments: an anatomic study. *J Bone Joint Surg Am*, 2002, 84: 2258–2265.
- Adams CR, DeMartino AM, Rego G, Denard PJ, Burkhart SS. The rotator cuff and the superior capsule: why we need both. *Art Ther*, 2016, 32: 2628–2637.
- Mall NA, Tanaka MJ, Choi LS, Paletta GA Jr. Factors affecting rotator cuff healing. *J Bone Joint Surg Am*, 2014, 96: 778–788.
- Ding DY, Ryan WE, Strauss EJ, Jazrawi LM. Chronic distal biceps repair with an Achilles allograft. *Arthrosc Tech*, 2016, 5: e525–e529.
- Läderrmann A, Denard PJ, Abrassart S, AJP S. Achilles tendon allograft for an irreparable massive rotator cuff tear with bony deficiency of the greater tuberosity. *Knee Surg Sports Traumatol Arthrosc*, 2017, 25: 2147–2150.
- Diniz P, Pacheco J, Flora M, et al. Clinical applications of allografts in foot and ankle surgery. *Knee Surg Sports Traumatol Arthrosc*, 2019, 27: 1847–1872.